an effect previously noted by other groups (*14, 15*).

These results suggest that the PtdIns(3,4,5)P_3 signal can be transduced by the actions of a PtdIns(3,4,5)P_3-activated protein kinase; thus, the regulation of this pathway is analogous to that of other signaling systems that respond to small molecule signals (adenosine 3′,5′-monophosphate–dependent protein kinase, protein kinase C, and Ca^{2+}/calmodulin-dependent protein kinases). In the PtdIns(3,4,5)P_3 pathway, the lipid signal controls PKB activity in two distinct but cooperative ways, which is reminiscent of the role of adenosine monophosphate (AMP) to allosterically activate the AMP-activated protein kinase, and also to activate the kinase that phosphorylates the AMP-activated protein (*24*). This may ensure tight regulation of PKB at the correct membrane localization, and it will be interesting to see whether this dual regulatory principle will apply to other targets in the PI3K signaling pathway.

Note added in proof: A PtdIns(3,4,5)P_3-dependent protein kinase has been purified (*25*) that may be related to the upstream kinase described here.

REFERENCES AND NOTES

1. S. P. Staal, *Proc. Natl. Acad. Sci. U.S.A.* **84**, 5034 (1987).
2. A. Bellacosa *et al*., *Oncogene* **8**, 745 (1993).
3. N. N. Ahmed *et al*., *ibid.*, p. 1957.
4. A. D. Kohn, F. Takeuchi, R. A. Roth, *J. Biol. Chem.* **271**, 21920 (1996).
5. M. A. Lemmon, K. M. Ferguson, J. Schlessinger, *Cell* **85**, 621 (1996).
6. B. M. T. Burgering and P. J. Coffer, *Nature* **376**, 599 (1995).
7. T. F. Franke *et al*., *Cell* **81**, 727 (1995).
8. A. D. Kohn, K. S. Kovacina, R. A. Roth, *EMBO J.* **14**, 4288 (1995).
9. A. Klippel *et al*., *Mol. Cell. Biol.* **16**, 4117 (1996); S. A. Didichenko, B. Tilton, B. A. Hemmings, K. Ballmer-Hofer, M. Thelen, *Curr. Biol.* **6**, 1271 (1996).
10. D. A. E. Cross, D. R. Alessi, P. Cohen, M. Andjelkovich, B. A. Hemmings, *Nature* **378**, 785 (1995).
11. T. F. Franke, D. R. Kaplan, L. C. Cantley, *Cell* **88**, 435 (1997).
12. D. R. Alessi *et al*., *EMBO J.* **15**, 6541 (1996).
13. S. R. James *et al*., *Biochem. J.* **315**, 709 (1996).
14. A. Klippel, W. M. Kavanaugh, D. Pot, L. T. Williams, *Mol. Cell. Biol.* **17**, 338 (1997).
15. T. F. Franke, D. R. Kaplan, L. C. Cantley, A. Toker, *Science* **275**, 665 (1997).
16. PSG5(HA)PKB was obtained from B. Burgering (Utrecht University, Utrecht, The Netherlands). The cDNA encoding PKB was subcloned into pBluescript, and phosphorylation site and PH domain mutants were obtained with a strategy based on the polymerase chain reaction [with the use of *Pfu* DNA polymerase (Stratagene) and low cycle numbers]. The ΔPH-PKB mutant lacks the first 125 amino acids. All mutations were checked by sequencing. The appropriate cDNAs were then subcloned into a mammalian expression vector [pCMV3(EE)] and a baculovirus transfer vector [pAcoG1(EE)] encoding NH_2-terminal EEEEFMPME (Glu-Glu) tags (*25*) (E, Glu; F, Phe; M, Met; P, Pro).
17. D. Stokoe, unpublished data.
18. L. R. Stephens, T. R. Jackson, P. T. Hawkins, *Biochim. Biophys. Acta* **1179**, 27 (1993).
19. Details of the synthesis of dipalmitoyl- and stearoyl-arachidonoyl PtdIns(3,4,5)P_3 and their isomers will be published separately.
20. Rat tissues (5 g) were homogenized in 5 volumes of 20 mM tris (pH 7.5), 1 mM EDTA, 25 mM NaF, 1 mM dithiothreitol (DTT), 1 mM NaVn, leupeptin (10 μg/ml), soybean trypsin inhibitor (10 μg/ml), aprotinin (10 μg/ml), and 100 μM pefabloc and centrifuged at 20,000*g* for 30 min to prepare cytosolic extracts. Extracts (~20 mg) were loaded onto a Mono Q column (Pharmacia) and the bound proteins eluted with a 20-ml gradient to 500 mM NaCl in the same buffer. We collected 1-ml fractions, and portions (10 μl) were added to 0.1 μg of purified recombinant Glu-Glu–tagged PKB, 5 mM $MgCl_2$, 2 mM ATP, and 1% NP-40 in a volume of 40 μl. The stearoyl-arachidonoyl PtdIns(3,4,5)P_3 (5 μM) was added as indicated. After 20 min at 30°C, the reactions were stopped by the addition of 10 mM EDTA, and the PKB was affinity-purified with an antibody to the Glu-Glu tag coupled to protein G–Sepharose beads. After washing the beads with tris-buffered saline (TBS) containing 1% NP-40 and 1 mM EDTA, we assayed the immobilized PKB in a volume of 30 μl with 50 μM "Crosstide" (GRPRTSSFAEG, a peptide based on the NH_2-terminus of GSK-3) as a substrate (A, Ala; E, Glu; F, Phe; G, Gly; P, Pro; R, Arg; S, Ser; T, Thr). The ability of each fraction to phosphorylate PKB was determined in a similar manner, except the concentration of ATP was reduced to 10 μM, and 2.5 μCi of [γ^{32}P]ATP was added to each assay. After affinity purification of the PKB, the beads were washed with TBS containing 1% NP-40 and 1 mM EDTA and then analyzed by SDS–polyacrylamide gel electrophoresis and autoradiography.
21. There are at least two potential reasons why the two peaks of phosphorylation and activation reproducibly do not exactly coincide. The Glu-Glu–tagged PKB from Sf9 cells purifies as a heterogeneous mixture of phosphoproteins that is partially active. These species may exhibit differences in their ability to become phosphorylated versus their ability to become activated. An alternative possibility is that there is a second activity eluting earlier in the gradient that is required in addition to phosphorylation of PKB for activation, and it is when both this peak and the kinase peak overlap that the activation of PKB is seen. The two peak fractions were pooled for subsequent analysis of this activity.
22. Radiolabeled peptides were sequenced in a Beckman 890C spinning cup sequenator in the presence of Polybrene and horse myoglobin. Each cycle fraction was blown dry in a chemical fume hood, redissolved in 6 ml of scintillation fluid and counted for 20 min, and corrected for background.
23. K. Datta, A. Bellacosa, T. O. Chan, P. N. Tsichlis, *J. Biol. Chem.* **271**, 30835 (1996).
24. S. Hawley *et al*., *ibid.* **270**, 27186 (1995).
25. D. R. Alessi *et al*., *Curr. Biol.* **7**, 261 (1997).
26. T. Grussenmeyer, K. H. Scheidtmann, M. A. Hutchinson, W. Eckhart, G. Walter, *Proc. Natl. Acad. Sci. U.S.A.* **82**, 7952 (1985); L. R. Stephens *et al*., *Cell* **89**, 105 (1997).

27. This research is supported in part by the National Cancer Institute, NIH, Department of Health and Human Services under contract with ABL. P. Hawkins is a Biotechnology and Biological Sciences Research Council Research Fellow. We thank B. Burgering for the PSG5(HA)PKB, E. Porfiri for critical reading of the manuscript and helpful suggestions, D. Morrison for helpful suggestions, and Bayer Corporation for interactive support.

25 March 1997; accepted 28 May 1997

Transmission of Hepatitis C by Intrahepatic Inoculation with Transcribed RNA

Alexander A. Kolykhalov, Eugene V. Agapov, Keril J. Blight, Kathleen Mihalik, Stephen M. Feinstone, Charles M. Rice*

More than 1% of the world's population is chronically infected with hepatitis C virus (HCV). HCV infection can result in acute hepatitis, chronic hepatitis, and cirrhosis, which is strongly associated with development of hepatocellular carcinoma. Genetic studies of HCV replication have been hampered by lack of a bona fide infectious molecular clone. Full-length functional clones of HCV complementary DNA were constructed. RNA transcripts from the clones were found to be infectious and to cause disease in chimpanzees after direct intrahepatic inoculation. This work defines the structure of a functional HCV genome RNA and proves that HCV alone is sufficient to cause disease.

In 1989, HCV, the viral agent believed to be responsible for most posttransfusion non-A, non-B hepatitis, was molecularly cloned (*1*). HCV is an enveloped positive-strand RNA virus classified in the family Flaviviridae (*2*). Characterization of HCV genome organization and expression has progressed rapidly since its discovery (*3*). The HCV genome RNA is ~9.6 kb and consists of a 5′ nontranslated region (NTR) that functions as an internal ribosome entry site, a long open reading frame (ORF) encoding a polyprotein of >3000 amino acids, and a 3′ NTR. The genome RNA was originally thought to terminate with polyadenylate [poly(A)] or polyuridylate [poly(U)] tracts, but recent studies have revealed the presence of an internal poly(U)/polypyrimidine [poly(U/UC)] tract followed by a highly conserved 98-base sequence (*4, 5*). The HCV polyprotein is processed by host signal peptidase and two viral proteinases to yield at least 10 different structural and nonstructural (NS) proteins (Fig. 1). Properties of many of the HCV-encoded replication enzymes, such as the serine proteinase, RNA helicase, and polymerase have begun to emerge as part of intensive efforts to devel-

A. A. Kolykhalov, E. V. Agapov, K. J. Blight, C. M. Rice, Department of Molecular Microbiology, Washington University School of Medicine, 660 South Euclid Avenue, St. Louis, MO 63110–1093, USA
K. Mihalik and S. M. Feinstone, Division of Virology, Center for Biologics Evaluation and Research, Food and Drug Administration, Bethesda, MD 20892, USA

*To whom correspondence should be addressed.

op new and more effective treatments for chronically infected HCV carriers. These efforts have been hampered, however, by poor replication in cell culture, the restricted host range of the virus (the chimpanzee, *Pan troglodytes*, is the only known nonhuman host), and the lack of an infectious molecular clone for genetic analysis of HCV functions.

Problems with constructing a functional HCV cDNA clone include the highly variable "quasi-species" nature of this RNA virus, the small quantities of viral RNA present in clinical samples, which necessitate in vitro amplification before cloning, and the lack of a simple and verified transfection assay for infectivity. As starting material, we used serum obtained from a patient in the early phase of infection (designated H77) (*6*). This high specific–infectivity serum contains ~10^8 RNA molecules and ~$10^{6.5}$ chimpanzee infectious doses per milliliter. A combinatorial library with a complexity of >10^5 full-length HCV cDNAs was constructed by high-fidelity assembly reverse transcription–polymerase chain reaction (RT-PCR) followed by subcloning into a recipient plasmid vector containing the 5′- and 3′-terminal HCV consensus sequences (*7*). A flanking T7 promoter and an engineered specific restriction site allowed for production of runoff RNA transcripts; 233 of the clones were prescreened by restriction analysis, polyprotein processing, and production of the COOH-terminal NS5B protein (the HCV RNA-dependent RNA polymerase). In an unsuccessful experiment, RNAs transcribed from 34 clones that passed these analyses were assayed for infectivity by direct intrahepatic injection in two HCV-naïve chimpanzees (*8*). As a negative control, a third animal received similar injections with transcripts from a clone containing a 20–amino acid in-frame deletion encompassing the NS5B polymerase active site. Serum samples were collected for 2 months after

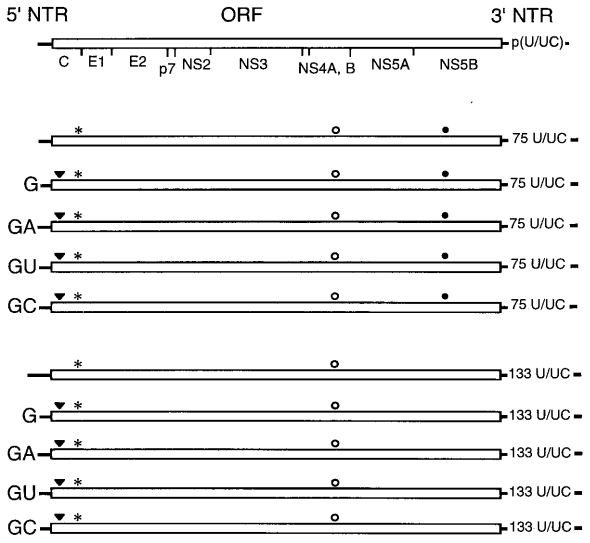

Fig. 1. Features of the 10 full-length consensus clone derivatives tested in chimpanzees. (**Top**) Schematic of HCV H77 cDNA consensus RNA. The 5′ and 3′ NTRs (solid lines) and the consensus ORF (open box) are indicated with the approximate locations of the polyprotein cleavage products shown below. (**Bottom**) The 10 RNA transcripts used for chimpanzee inoculation are diagrammed. Additional 5′ nucleotides and 75-base versus 133-base poly(U/UC) tracts are indicated. All clones and transcripts included two silent nucleotide substitutions: position 899 (C instead of U, asterisks); position 5936 (C instead of A, open circles) (nucleotide positions refer to the HCV H sequence). The substitution at position 5936 inactivated an internal Bsm I site in the H77 cDNA sequence so that an engineered Bsm I site could be used for production of runoff RNA transcripts with the exact 3′ terminus of HCV genome RNA (*15*). Clones with additional 5′ bases contained a silent marker mutation inactivating the Xho I site at position 514 (solid triangles). Clones with 75-base versus 133-base poly(U/UC) tracts were distinguished by A (solid circles) versus G at position 8054, respectively. The 10 derivatives were created by standard recombinant DNA methods and their structures were verified by restriction digestion and sequence analysis.

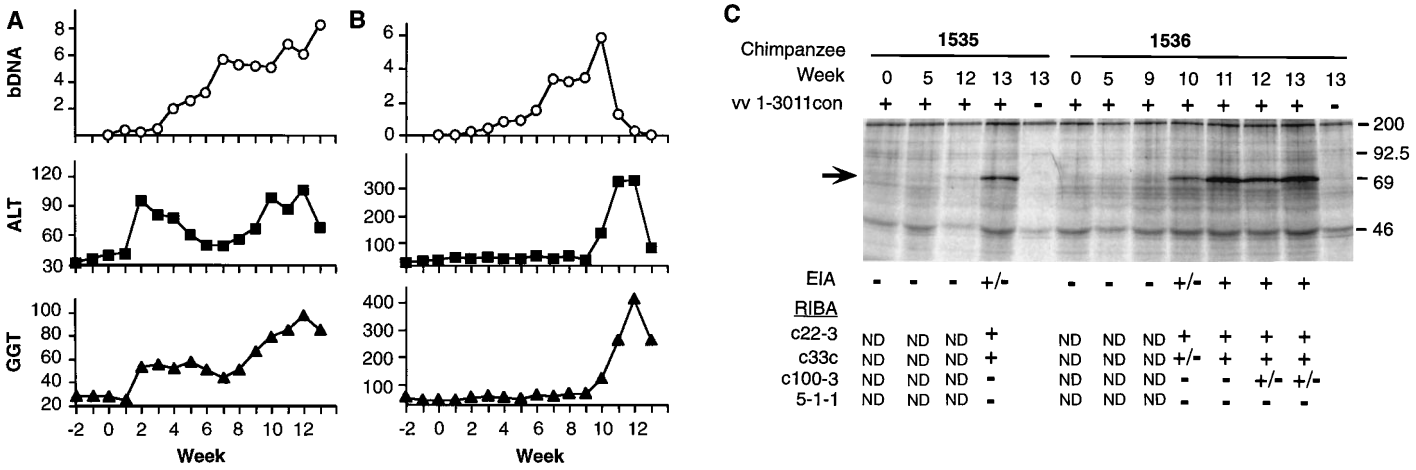

Fig. 2. Viremia, hepatitis, and serologic response in chimpanzees inoculated with transcribed RNA. Before and after inoculation, animals were monitored weekly for the amount of circulating HCV RNA, liver transaminases, and HCV-specific antibodies. RNA and liver enzyme data are shown for chimpanzees 1535 (**A**) and 1536 (**B**). RNA was quantified by the bDNA assay (Chiron Corp.) and is reported as mega equivalents of RNA per milliliter (Meq/ml) (detection limit is 0.2 Meq/ml). Liver enzymes measured included serum alanine aminotransferase (ALT) (indicated in IU/liter) and γ-glutamyltransferase (GGT) (IU/liter). Normal ALT and GGT concentrations range from 18 to 45 and from 0 to 60 IU/liter, respectively. (**C**) HCV-specific serologic responses (+) were detected by commercial enzyme immunoassay (EIA) and recombinant immunoblot assay (RIBA) (*17*) as well as by immune precipitation of metabolically labeled HCV antigens (*23*). Only EIA-positive samples were analyzed by RIBA (ND, not determined). For the immunoprecipitation analyses, radioactively labeled HCV antigens were produced by infection of BHK-21 cells with a vaccinia recombinant expressing the entire HCV H77 consensus polyprotein (vvHCV 1-3011con) [(*9*); see also (*23*)]. Cells were lysed in TNA [0.5% Triton X-100, 200 mM NaCl, 50 mM tris-HCl (pH, 7.4), 1 mM EDTA, 1 mg of bovine serum albumin per milliliter, and 20 μg of phenylmethylsulfonyl fluoride per milliliter], clarified, and incubated with 2.5 μl of chimpanzee serum followed by 3 μl of rabbit antibody to human immunoglobulin. Immunoprecipitates were collected, washed, and separated by electrophoresis on a SDS–12% polyacrylamide gel. HCV NS3 was present in the 70-kD species immunoprecipitated by the chimpanzee sera (arrow) as shown by solubilizing the immunoprecipitates (in 2% SDS, 1% 2-mercaptoethanol, and 20 mM DTT, and heating at 80°C for 20 min), diluting the eluted proteins with 20 volumes of TNA, and reprecipitating with an HCV NS3-specific rabbit polyclonal antiserum (*9, 23*).

inoculation and analyzed for evidence of HCV replication. Neither experimental animal nor the negative control animal exhibited signs of productive infection (circulating HCV RNA, increased liver enzymes, histopathology, or seroconversion) (*9*). Of note was the absence of detectable circulating HCV RNA 2 days after inoculation.

Missing terminal sequences, low RNA transfection efficiencies in vivo, and errors introduced during cDNA synthesis or PCR amplification might account for these negative results. Because the latter concern was readily addressed, we sequenced six clones from the combinatorial library, as well as uncloned RT-PCR products, to determine a consensus sequence for the H77 isolate (*10*). From this analysis, it became apparent that each of the six clones sequenced contained numerous non–consensus sequence changes scattered throughout the genome, which could be deleterious and would explain the negative results. We used this information to direct the assembly of a full-length clone reflecting the H77 consensus sequence (*11*). Aside from the sporadic changes corrected in this consensus clone, even greater sequence heterogeneity was noted in three regions of the HCV genome. During analysis of the extreme 5′ terminus, we found a substantial number of clones that contained one or more bases in addition to the reported 5′-terminal sequence (5′-GCCAG . . . -3′) (*12*). In the structural protein coding region, the NH_2-terminus of the E2 virion envelope glycoprotein was highly variable, but a predominant sequence was identified (*13*). Near the 3′ terminus, the poly(U/UC) tract was variable in length and composition (*14*). Because these differences might be functionally significant, variants of the consensus clone with additional bases at the 5′ terminus and two different poly(U/UC) tracts were constructed (Fig. 1). Silent nucleotide substitutions were engineered as markers so that virus recovered from transfected animals could be sequenced to identify which clones were infectious.

From each of the 10 clones, full-length uncapped RNAs were transcribed from linearized template DNAs (*15*) and used for inoculation of two chimpanzees that were seronegative for all known hepatitis viruses, were negative for HCV RNA by nested RT-PCR, and had normal baseline amounts of liver enzymes. Animals were inoculated by direct intrahepatic injection at multiple sites (*16*). Serum samples and liver biopsies were taken before inoculation and at weekly intervals thereafter. For 3 months after inoculation, serum samples were assayed for liver enzymes, antibodies to HCV, and viremia, as assessed by quantifying circulating HCV RNA by branched DNA (bDNA) and quantitative-competitive (QC) RT-PCR (*5*).

Chimpanzee 1535 had increased concentrations of serum alanine aminotransferase (ALT), which is a marker for liver damage, at week 2 after inoculation; ALT gradually declined to the preinoculation baseline amount and then increased again in weeks 10 to 12 (Fig. 2A). HCV RNA titers were undetectable before inoculation, increased to 0.45 Meq/ml by week 1, decreased slightly at week 2 (0.28 Meq/ml), and then continued to climb steadily, reaching 8.3 Meq/ml by week 13. This animal became clearly HCV seropositive at week 13 (Fig. 2C) (*17*). Chimpanzee 1536 showed no evidence of early liver damage (Fig. 2B). At week 10, ALT concentrations increased sharply and peaked at week 12, declining rapidly thereafter. At week 1, the HCV RNA titer was undetectable by bDNA (detection limit, 0.2 Meq/ml or ~2×10^5 RNA molecules per milliliter), but 10^4 RNA molecules per milliliter were measured by QC RT-PCR. The circulating HCV RNA titer peaked at week 10 (5.8 Meq/ml) and then declined to quantities undetectable by bDNA by week 13. Chimpanzee 1536 had seroconverted by week 10 (Fig. 2C). Histologic changes in liver biopsies were typical for hepatitis C in chimpanzees (*18*) and were characterized predominantly by portal inflammation and focal necrosis. Hepatocyte alterations included multinucleated hepatocytes, cytoplasmic clumping, and vacuolization probably representing fat droplets (*9*). The severity of histologic lesions appeared generally to parallel the ALT elevations. These pathogenesis profiles are strikingly reminiscent of those obtained in chimpanzees inoculated with the infectious H77 material or other HCV-containing samples (*19*).

To prove that the signals detected in the bDNA and QC RT-PCR assays were not due to residual template DNA from the transcription reactions, we assayed all the samples by PCR without reverse transcription. No products were obtained, which demonstrated that the signals detected were due to HCV RNA (Fig. 3A). If the HCV RNA detected in serum were from replicating virus, RNAs should be packaged in enveloped virions and resistant to degradation by ribonuclease (RNase), whereas residual transcript RNA should be RNase-sensitive. Indeed, the HCV RNA in samples of chimpanzee serum was resistant to RNase digestion under conditions that completely degraded excess naked competitor RNA (Fig. 3B). Moreover, there was no

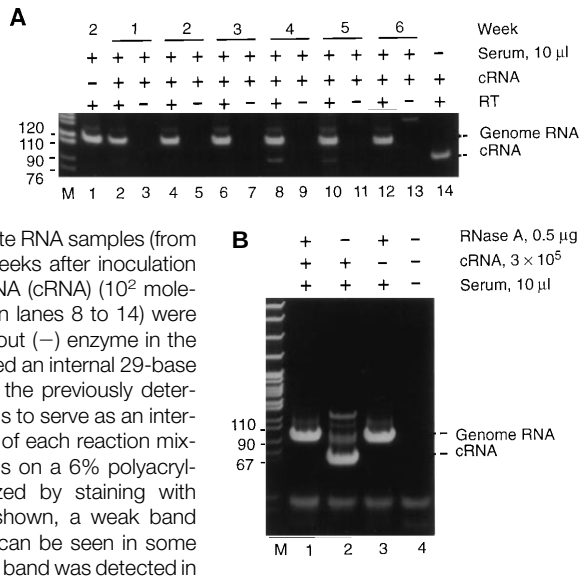

Fig. 3. Circulating HCV nucleic acid is RNA and is RNase resistant. (**A**) Serum samples from inoculated animals do not contain carryover template DNA. The analysis shown is for chimpanzee 1535, which received the largest amount of inoculated HCV RNA and where the template DNA had not been degraded by digestion with DNase I (*16*). Duplicate RNA samples (from 10 μl of serum) from the indicated weeks after inoculation without (lane 1) or with competitor RNA (cRNA) (10^2 molecules in lanes 2 to 7; 10^3 molecules in lanes 8 to 14) were amplified by RT-PCR with (+) or without (−) enzyme in the RT step (*5*). The cRNA, which contained an internal 29-base deletion, was added at 1/10 to 1/30 the previously determined HCV nucleic acid concentrations to serve as an internal RT-PCR control. An equal portion of each reaction mixture was separated by electrophoresis on a 6% polyacrylamide gel and bands were visualized by staining with ethidium bromide. In the exposure shown, a weak band corresponding to the cRNA product can be seen in some lanes (such as lane 8). No specific PCR band was detected in the absence of cDNA synthesis, indicating that the HCV-specific nucleic acid signal was due to RNA. (**B**) Circulating HCV RNA from inoculated animals is protected from RNase. The sample analyzed was week 6 serum from chimpanzee 1536, which had an HCV RNA titer of 6×10^6 molecules per milliliter by QC RT-PCR. Extracted RNA samples were subjected to nested RT-PCR (*5*) and an equal portion of each reaction mixture was separated by electrophoresis on a 6% polyacrylamide gel. Lane 1, 10 μl of serum (containing ~6×10^4 HCV RNA molecules) was mixed with excess cRNA (3×10^5 molecules), digested with 0.5 μg of RNase A for 15 min at room temperature, and extracted with RNAzol. Lane 2, 10 μl of serum was first extracted with RNAzol and then mixed with 3×10^5 molecules of cRNA. Lane 3, 10 μl of serum without added cRNA was predigested with RNase A and then extracted with RNAzol. Lane 4, negative control for RT-PCR. The RT-PCR products corresponding to HCV genomic and cRNA are indicated. In lane 2, the relative intensity of the genomic and cRNA products reflects the approximately fivefold difference in the molar amounts of these RNAs in this competitive RT-PCR reaction. The additional band of higher apparent molecular mass represents a heteroduplex of the genomic and cRNA PCR products, see (*5*).

correlation between the level of apparent viremia and the amount of inoculated RNA. The total amount of transcript RNA used for inoculation of chimpanzee 1535 was ~3000 μg but it was only ~22 μg for chimpanzee 1536. Despite this ~150-fold difference, similar levels of viremia were observed (Fig. 2). Finally, in two previous animal experiments (a total of six animals), circulating HCV-specific nucleic acid was never detected, even as early as 2 days after inoculation (9). These experiments suggested that circulating RNA was a result of authentic virus replication rather than release of inoculated nucleic acid.

Restriction enzyme digestion and sequence analysis of recovered viral RNA revealed the presence of engineered markers, proving that these infections stemmed from the inoculated transcript RNAs. Two silent mutations at position 899 (C instead of T) and at position 5936 (C instead of A, which ablated the internal Bsm I site at position 5934), marked all the transfected RNAs (Fig. 1). For the nucleotide (nt) 899 marker, the region between nt 466 and nt 950 was amplified by nested RT-PCR, sequenced directly, and found to have the expected H77 consensus sequence except for the engineered C marker at nt 899 (9). The region from nt 5801 to 6257 was also amplified by nested RT-PCR and was found to be resistant to digestion with Bsm I but not to four other enzymes known to cleave in that region (9). These analyses were conducted for both chimpanzee 1535 (week 5) and chimpanzee 1536 (week 6).

Additional silent markers were analyzed to identify the 5′-terminal sequence(s) and the length(s) of poly(U/UC) tract required or preferred for initiating infection (*20*, *21*). Although it is not possible to draw firm quantitative conclusions about differences in specific infectivity, the results clearly demonstrated that the RNA transcripts without any additional 5′ nucleotides were infectious (*20*). Transcripts with additional 5′ nucleotides could also initiate infection, although our analysis did not allow us to distinguish among the various derivatives tested (Fig. 1). Transcripts containing either the 75-base or the 133-base poly(U/UC) tracts were infectious, but the 133-base poly(U/UC) tract was preferred (*21*).

The demonstration that RNA transcribed from cloned HCV cDNA can initiate infection and cause hepatitis in transfected chimpanzees provides formal proof (*22*) that HCV alone is the causative agent of this disease. With this model, HCV infection can now be launched from clonal derivatives to facilitate studies on virus evolution, pathogenesis, and host immune response relevant to understanding the factors that determine viral clearance versus chronic infection. Our experiments also define the elements of functional HCV genome RNA. Aside from a consensus genome sequence, no additional 5′ sequences were required for infectivity and 3′ poly(U/UC) tracts of variable length were tolerated. Infectious HCV RNAs can now be produced in unlimited quantities and used to identify and optimize cell-culture replication systems and to begin genetic analyses of HCV replication in vivo and in vitro.

REFERENCES AND NOTES

1. Q.-L. Choo *et al.*, *Science* **244**, 359 (1989).
2. C. M. Rice, in *Fields Virology*, B. N. Fields, D. M. Knipe, P. M. Howley, Eds. (Lippincott-Raven, Philadelphia, PA, 1996), vol. 1, pp. 931–960.
3. M. Houghton, *ibid.*, pp. 1035–1058; M. E. Major and S. M. Feinstone, *Hepatology* **25**, 527 (1997); K. E. Reed and C. M. Rice, in *Hepatitis C Virus*, H. W. Reesink, Ed. (Karger, Basel, Switzerland, 1997), vol. 61, in press.
4. T. Tanaka, N. Kato, M.-J. Cho, K. Shimotohno, *Biochem. Biophys. Res. Comm.* **215**, 744 (1995); T. Tanaka, N. Kato, M.-J. Cho, K. Sugiyama, K. Shimotohno, *J. Virol.* **70**, 3307 (1996); N. Yamada *et al.*, *Virology* **223**, 255 (1996).
5. A. A. Kolykhalov, S. M. Feinstone, C. M. Rice, *J. Virol.* **70**, 3363 (1996).
6. H. J. Alter, R. H. Purcell, P. V. Holland, H. Popper, *Lancet* **i**, 459 (1978); S. Feinstone *et al.*, *J. Infect. Dis.* **144**, 588 (1981); Y. K. Shimizu, R. H. Purcell, H. Yoshikura, *Proc. Natl. Acad. Sci. U.S.A.* **90**, 6037 (1993).
7. We screened 41 HCV primer pairs and found 11 sets useful for amplifying overlapping 1- to 4-kb portions of the H77 genome RNA [A. A. Kolykhalov, K. E. Reed, C. M. Rice, in *Hepatitis C Protocols*, J. Y. N. Lau, Ed. (Humana Press, Totowa, NJ), in press]. A mixture of thermostable enzymes was used to reduce error frequency and enhance synthesis of full-length products [W. M. Barnes, *Proc. Natl. Acad. Sci. U.S.A.* **91**, 2216 (1994); K. S. Lundberg *et al.*, *Gene* **108**, 1 (1991)]. With sequential rounds of assembly PCR, and a limited number of amplification cycles, intermediate PCR products were combined to produce nearly full-length HCV cDNA (nt 39 to 9352), which was cloned as a Kpn I (580)–Not I (9219) fragment into a recipient plasmid. This plasmid contained the T7 promoter, the consensus HCV-H 5′- and 3′-terminal sequences 5′ to the Kpn I site and 3′ from the Not I site, and a specific restriction site for template linearization and production of runoff RNA transcripts.
8. Seventeen clones were injected per animal by essentially the same procedures, which were eventually successful (*16*). Intrahepatic inoculation with RNA has been used successfully to initiate infection for two positive-strand RNA viruses: hepatitis A virus [S. U. Emerson *et al.*, *J. Virol.* **66**, 6649 (1992)] and rabbit hemorrhagic disease virus [V. F. Ohlinger, B. Haas, G. Meyers, F. Weiland, H.-J. Thiel, *ibid.* **64**, 3331 (1990)].
9. A. A. Kolykhalov *et al.*, unpublished data.
10. As will be reported elsewhere (A. A. Kolykhalov and C. M. Rice, in preparation), the HCV H77 consensus sequence (GenBank accession number AF009606) was determined by sequencing of six clones from the H77 combinatorial library (clones 12, 209, 211, 213, 227, and 248) (*7*), and selected regions amplified by RT-PCR.
11. Fragments produced by restriction digestion of the sequenced clones (*10*) were used to assemble a full-length consensus clone by standard methods. They were derived from the following regions and clones (in parentheses): nt 580–1045 (213); 1046–1173 (248); 1174–1356 (12); 1357–1481 (209); 1482–1747 (227); 1748–1907 (209); 1908–2107 (227); 2108–2321 (12); 2322–2439 [HCV-H prototype, as described in (*23*)]; 2440–2525 (213); 2526–2827 (HCV-H prototype); 2828–2977 (211); 2978–3235 (209); 3236–3477 (227); 3478–3732 (209); 3733–3941 (12); 3942–4068 (211); 4069–4544 (227); 4545–4645 (248); 4646–4975 (211); 4976–5609 (227); 5610–5749 (209); 5750–6208 (HCV-H prototype); 6209–6301 (213); 6302–7528 (227); 7529–7860 (213); 7861–8204 (209); 8205–9219 (213).
12. Both the cDNA cyclization and inverse PCR and oligonucleotide–cDNA ligation (5′ rapid amplification of cDNA ends) methods were used to determine the 5′-terminal sequence of HCV RNA from high-titer H77 plasma (*10*). The predominant sequence, 5′-GCCAGCC . . . -3′, was identical to that determined for most other HCV isolates. Less frequently, clones with additional 5′ bases (including G, U, A, AA, GC, GG, GGG, and AAAGTCC) were recovered.
13. The NH_2-terminal portion of E2 (HVR1) is highly variable and believed to be the target of immune selection (*3*). In the H77 sample, considerable variability exists in HVR1 [N. Nakajima, M. Hijikata, H. Yoshikura, Y. K. Shimizu, *J. Virol.* **70**, 3325 (1996); N. Ogata, H. J. Alter, R. H. Miller, R. H. Purcell, *Proc. Natl. Acad. Sci. U.S.A.* **88**, 3392 (1991); G. Inchauspe *et al.*, *ibid.*, p. 10292]. We sequenced multiple independent clones from this region (*10*) and the predominant HVR1 sequence in each position was used in our consensus clones.
14. The length and composition of the HCV 3′ NTR poly(U/UC) tract have not been determined unambiguously. Sufficient quantities of double-stranded cDNA could not be obtained from H77 serum for direct cloning of this region without resorting to PCR amplification, which can alter the length of the poly(U/UC) tract (*9*). Clones resulting from this procedure therefore may not reflect the native HCV genome RNA structure. In multiple independent clones derived by PCR amplification, the length of this tract varied from 41 to 133 nt (*5*). Hence, two different lengths of poly(U/UC) tract were tested: 75 and 133 bases. The length of the 75-base tract (from clone H77#8) (*5*) is actually about the medium length for all sequences (from different genotypes) reported by us or others (*4, 5*). The 133-base tract was recovered in only one HCV-H clone (H77#10) (*5*); a tract of similar length was recovered in one clone of a genotype 4 isolate (*5*). Such long poly(U/UC) tracts have not yet been reported by others (*4*).
15. Purified plasmid DNAs were digested to completion with Bsm I, extracted once with phenol-chloroform, and precipitated with ethanol. DNA pellets were washed with ethanol to remove salts and resuspended in H_2O. Transcription reaction mixtures (120 μl) contained the following components: 12 μg of linearized template DNA, 40 mM tris-HCl (pH 7.8), 16 mM $MgCl_2$, 5 mM dithiothreitol (DTT), 10 mM NaCl, 3 mM each NTP, 100 units of T7 RNA polymerase, and 0.02 unit of inorganic pyrophosphatase. After 1 hour of incubation at 37°C, typical yields were about 350 μg with >80% full-length RNA, as estimated by gel electrophoresis (*9*).
16. Two different inoculation and transfection protocols were used. For chimpanzee 1535, 100 μl of each transcription reaction mixture was diluted with 400 μl of phosphate-buffered saline (PBS) and stored frozen at −80°C until used for inoculation. These storage conditions were tested and shown to have no observable effect on the integrity of HCV RNA transcripts. Before inoculation, samples were thawed and each sample was injected intrahepatically at two sites (~0.25 ml per site). Injection sites for the 10 clones were distributed in three lobes of the liver. Chimpanzee 1536 was inoculated with smaller amounts of RNA that had been mixed with lipofectin (Bethesda Research Labs). In this case, 20 μl of the same transcription reaction mixtures of the 10 full-length HCV H77 templates was treated with deoxyribonuclease (DNase I) to remove template DNA; 0.15-μg, 0.5-μg, and 1.5-μg portions were diluted to 50 μl with PBS and stored at −80°C until used for inoculation. After the mixtures were thawed, 100 μl of PBS containing 9 μg of lipofectin was added to each sample, mixed, and

injected into a single site. Hence, each transcript preparation, with different RNA/lipofectin ratios, was injected at three separate sites. The chimpanzees were caged and maintained under conditions that met all relevant requirements for the use of primates in an approved facility. Animal protocols were reviewed and approved by the animal care and use committees from each institution involved with the chimpanzee studies. The chimpanzee experiments were also reviewed and approved by the Public Health Service Interagency Animal Model Committee.

17. Antibodies to HCV were measured by commercial enzyme immunoassays. The Abbott HCV EIA 2.0 assay (Abbott Laboratories, Abbot Park, IL) contains three recombinant HCV antigens: HC34, polyprotein amino acid residues 1 to 150 (HCV core protein); HC-31, residues 1192 to 1457 (an internal portion of NS3) and residues 1676 to 1931 (COOH-terminus of NS4A and most of NS4B); and c100-3, residues 1569 to 1931 (the COOH-terminal portion of NS3, NS4A, and most of NS4B). Antigen-specific reactivity of EIA-positive sera was further defined with the strip immunoblot assay RIBA HCV 2.0 SIA (Chiron Corporation, Emeryville, CA), which contains four recombinant antigens: c22-3, residues 2 to 120 (HCV core protein); c33c, residues 1192 to 1457 (internal region of NS3); c100-3; and 5-1-1, residues 1694 to 1735 (COOH-terminal portion of NS4A and NH_2-terminal portion of NS4B). Tests were performed according to the manufacturer's directions.
18. H. Popper, J. L. Dienstag, S. M. Feinstone, H. J. Alter, R. H. Purcell, *Virchows Arch. A Pathol. Anat. Histol.* **387**, 91 (1980).
19. P. Farci *et al.*, *J. Infect. Dis.* **165**, 1006 (1992); M. Shindo, A. M. DiBisceglie, R. Biswas, K. Mihalik, S. M. Feinstone, *ibid.* **166**, 424 (1992).
20. The small amounts of circulating HCV RNA preclude direct determination of 5′-terminal RNA sequences. Therefore, virus derived from transcripts containing the most prevalent 5′ end (5′-GCCA . . . -3′) was distinguished from that derived from transcripts with additional 5′ nucleotides by the presence or absence of the Xho I site at position 514 (Fig. 1). The region containing this marker was amplified by RT-PCR under conditions that ensured that a representative number of independent cDNAs [A. A. Kolykhalov, K. E. Reed, C. M. Rice, in *Hepatitis C Protocols*, J. Y. N. Lau, Ed. (Humana Press, Totowa, NJ), in press] were analyzed (>50 in this case). The resulting products were analyzed for digestion with either Xho I or, as a control, Acc I, an enzyme that should digest this fragment for all input clones. For chimpanzee 1535 (week 3 sample), the fraction of products digested by excess Xho I paralleled the input inoculum: about 20% was digested by Xho I; 80% was resistant to digestion (values were determined by scanning ethidium bromide–stained digestion patterns with an IS-1000 Digital Imaging System, Alpha Innotech Corp.). Complete digestion was observed for Acc I. In the week 4 sample analyzed for chimpanzee 1536, 45% was digested by Xho I; 55% was resistant to digestion. Again, complete digestion was observed for Acc I. Thus, in chimpanzee 1536 an advantage was observed for transcripts without additional 5′ bases (5′-GCCA . . . -3′).
21. Transcripts containing 75-base or 133-base poly(U/UC) tracts were distinguished by the silent marker at nt 8054 in the NS5B coding region (Fig. 1). The region between nt 7955 and 8088 was amplified by RT-PCR, with enough starting material to ensure amplification of >100 independent cDNA molecules [A. A. Kolykhalov, K. E. Reed, C. M. Rice, in *Hepatitis C Protocols*, J. Y. N. Lau, Ed. (Humana Press, Totowa, NJ, in press)], and molecularly cloned. Sequences of 10 and 9 independent clones were determined for chimpanzee 1535 (week 3) and chimpanzee 1536 (week 4), respectively. It was found that 90% (chimpanzee 1535) and 67% (chimpanzee 1536) of the clones contained the G at nt 8054, indicative of the 133-base poly(U/UC) tract. Thus, the 133-base tract appears to be preferred, although we cannot rule out the possibility that this preference was because of a deleterious effect of the marker mutation on the transcripts with the 75-base tract.
22. S. Falkow, *Rev. Infect. Dis.* **10** (Suppl. 2), S274 (1988).
23. A. Grakoui, C. Wychowski, C. Lin, S. M. Feinstone, C. M. Rice, *J. Virol.* **67**, 1385 (1993).
24. We thank C. Read for expert technical assistance, S. Emerson for positive control hepatitis A virus cDNA clones, R. Purcell for generously making available his primate facilities, M. Shapiro for collection and analysis of chimpanzee samples, and A. DiBisceglie for bDNA analyses. We are also grateful to A. Grakoui, M. Heise, and J. A. Lemm for their participation in the early phases of this work and to S. Amberg, D. Goldberg, S. Hultgren, B. Lindenbach, M. MacDonald, J. Majors, and K. Reed for helpful discussion and comments on the manuscript. This work was supported in part by grants from the Public Health Service to C.M.R. (CA57973 and AI40034).

16 April 1997; accepted 19 June 1997

Mitosis in Living Budding Yeast: Anaphase A But No Metaphase Plate

Aaron F. Straight,* Wallace F. Marshall, John W. Sedat, Andrew W. Murray

Chromosome movements and spindle dynamics were visualized in living cells of the budding yeast *Saccharomyces cerevisiae*. Individual chromosomal loci were detected by expression of a protein fusion between green fluorescent protein (GFP) and the Lac repressor, which bound to an array of Lac operator binding sites integrated into the chromosome. Spindle microtubules were detected by expression of a protein fusion between GFP and Tub1, the major alpha tubulin. Spindle elongation and chromosome separation exhibited biphasic kinetics, and centromeres separated before telomeres. Budding yeast did not exhibit a conventional metaphase chromosome alignment but did show anaphase A, movement of the chromosomes to the poles.

The reproduction of eukaryotic cells depends on the ability of the mitotic spindle to segregate the replicated chromosomes into two identical sets. As cells enter mitosis they organize microtubules into a bipolar spindle. In most eukaryotes the kinetochore, a specialized region of the chromosome, binds microtubules, and in higher eukaryotes the condensed chromosomes move to a position equidistant from the spindle poles called the metaphase plate. Once all sister chromatids are properly aligned in metaphase, the linkage between the sister chromatids is dissolved, causing two changes that segregate the sisters from each other: Chromosomes move toward the spindle pole (anaphase A), and elongation of the spindle separates the spindle poles (anaphase B).

Knowledge of mitosis comes from three sources: microscopic observation and manipulation of animal and plant cells (*1*), studies in cell cycle extracts (*2*), and genetic analysis, especially in budding and fission yeast (*3*). To integrate the findings of these different approaches, we need to know if the basic features of mitosis are conserved among eukaryotes. Although the budding yeast *Saccharomyces cerevisiae* is an excellent organism for genetic analysis, its mitotic spindle is small and difficult to see in living cells. Individual mitotic yeast chromosomes are not visible by conventional light or electron microscopy and can only be seen by in situ hybridization to fixed cells (*4*, *5*). We have simultaneously visualized the mitotic spindle and individual chromosomes in living yeast cells. These studies show that (i) budding yeast chromosomes do not align on a metaphase plate, (ii) spindle elongation and chromosome separation exhibit biphasic kinetics, (iii) yeast exhibit anaphase A chromosome-to-pole movement, (iv) chromosomes are under poleward force as they separate, and (v) centromeres separate before telomeres.

We used green fluorescent protein (GFP) (*6*) to follow chromosome and spindle movements in living yeast cells by fluorescence microscopy. We visualized the spindle with a protein fusion between GFP and the major alpha tubulin (Tub1) (*7*). Specific loci were marked by binding of a protein fusion between GFP and the Lac repressor (GFP-LacI) to an integrated array of the Lac operator (LacO) (*8*, *9*). We observed synchronized cells passing through mitosis, taking vertical stacks of images every 26 s and subjecting them to iterative deconvolution (*10*, *11*). The top panel of Fig. 1A shows a series of optical sections after deconvolution projected as a stereo pair to reveal the structure of the entire spindle and the staining of the centromeres

A. F. Straight and A. W. Murray, Department of Physiology, Box 0444, School of Medicine, University of California at San Francisco, San Francisco, CA 94143–0444, USA.
W. F. Marshall and J. W. Sedat, Department of Biochemistry, Box 0448, School of Medicine, University of California at San Francisco, San Francisco, CA 94143–0448, USA.
*To whom correspondence should be addressed.

Transmission of Hepatitis C by Intrahepatic Inoculation with Transcribed RNA

Alexander A. Kolykhalov, Eugene V. Agapov, Keril J. Blight, Kathleen Mihalik, Stephen M. Feinstone and Charles M. Rice

Science **277** (5325), 570-574.
DOI: 10.1126/science.277.5325.570